Karlsruhe Institute of Technology
Department of Chemical and Process Engineering
Engler-Bunte-Institute
Division of Combustion Technology
Prof. Dr.-Ing. Henning Bockhorn

Numerical Investigation of the CFI Burner

Second Complementary Report

Prof. Dr.-Ing. Henning Bockhorn
Dr.-Ing. Feichi Zhang
B.Sc. Thorsten Zirwes

February 4, 2016

Contents

1 Introductory Remarks

In a first report, dated from June 10th 2015, preliminary results for the simulation of the CFI burner have been presented. The simulations have been performed with the commercial software ANSYS CFX 5. This program implements the methods of Computational Fluid Dynamics (CFD) and has been used for a wide range of fluid-flow problems for over 20 years. In the first report the mathematical basis to describe fluid motions and combustion processes have been presented. Furthermore, the report contained a brief description how the turbulent fluctuations of the fluid and the chemical reactions have been modeled in the CFX program, and what models were chosen for the simulation. In addition, a quick overview over the numerical methods used to discretize and solve the system of differential equations has been given, as well as an overview over the computational grid. Finally, results of selected simulations of the burner for different modes of operation were given.

The simulations presented in this first former report served to validate the applied methods and to obtain a first impression of the flow field and combustion in the CFI burning chamber. Due to this objectives, the operating conditions (e.g. thermal power, volume flows, kind of fuel etc.) of the burner used for the simulations did not coincide with the operating conditions applied in the development of the various actually realized versions of the CFI burning chamber.

In a second report, dated from October 20th 2015 a first step to approach one actually realized version of the CFI burning chamber by modifying the operating conditions and boundary conditions for the simulations has been performed. The geometry used for the simulations described in the second report is given in figure 1.
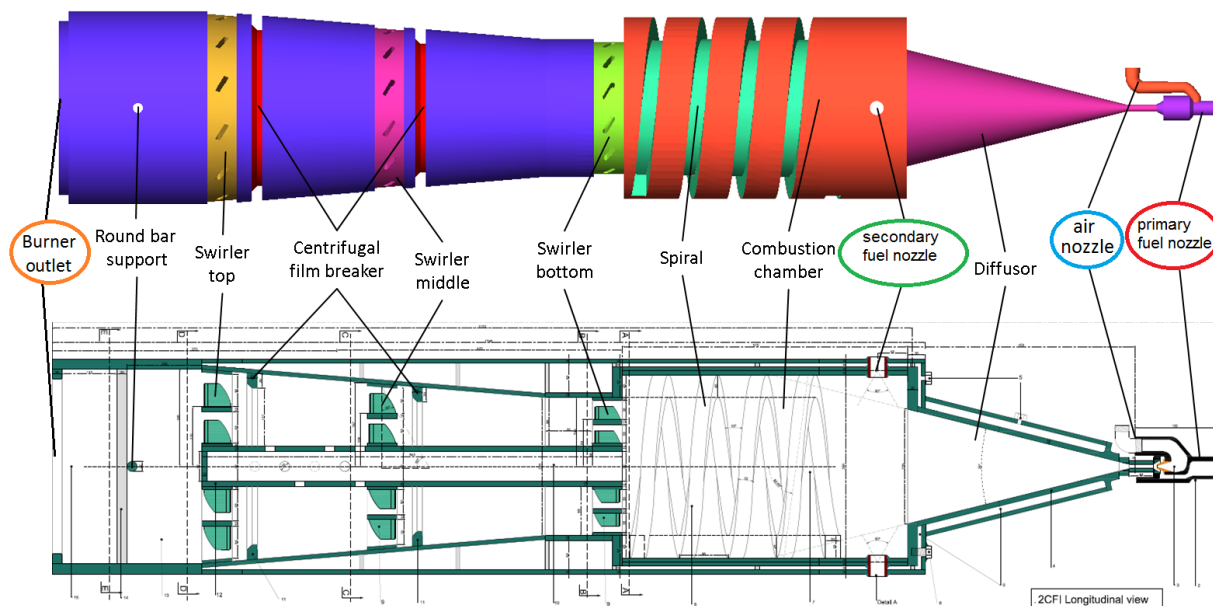

Figure 1: *Longitudinal view of the burner geometry used for the simulations in the second report dated from October 20th 2015 (denoted setup D). There are three types of inlets into the burner: the primary fuel nozzle (red circle), the air nozzle (blue circle) and the secondary fuel nozzles (side inlets, green circle). The Reynolds number of the burner used in the description of the numerical setup is based on the burner outlet (orange circle)*

The boundary conditions for the simulations described in the second report are given in the Table 1. One prescription is the pressure of about 30 bar in inlet pressure for the air nozzle. With the dimension of the air inlet nozzle (4 mm diameter) this results in the indicated air flow of about 0.122 kg/s. No fuel is fed through the primary fuel nozzle. The mass flow of methane through the secondary fuel nozzles (0.0065 kg/s) is adjusted to obtain over all slightly air-rich commbustion (equivalence ratio of 0.92). By this a thermal power of 325 kW is realized. A

second prescription has been the pressure at the outlet, which is ambient pressure (1 bar). This setup has been denoted "'setup D'" in continuation of the setups described in the report dated from June 10th 2015.

Table 1: *Pressures and mass flows entering the CFI burner for setup D.*

	T [K]	Composition	Flow Rate [kg/s]	Pressure [bar]
Air Nozzle	300	$Y_{O_2} = 0.233$, $Y_{N_2} = 0.767$	0.122	30
Primary fuel Nozzle	300	$Y_{CH_4} = 1$	0.0	–
Secondary fuel nozzle	383	$Y_{CH_4} = 1$	0.0065	1

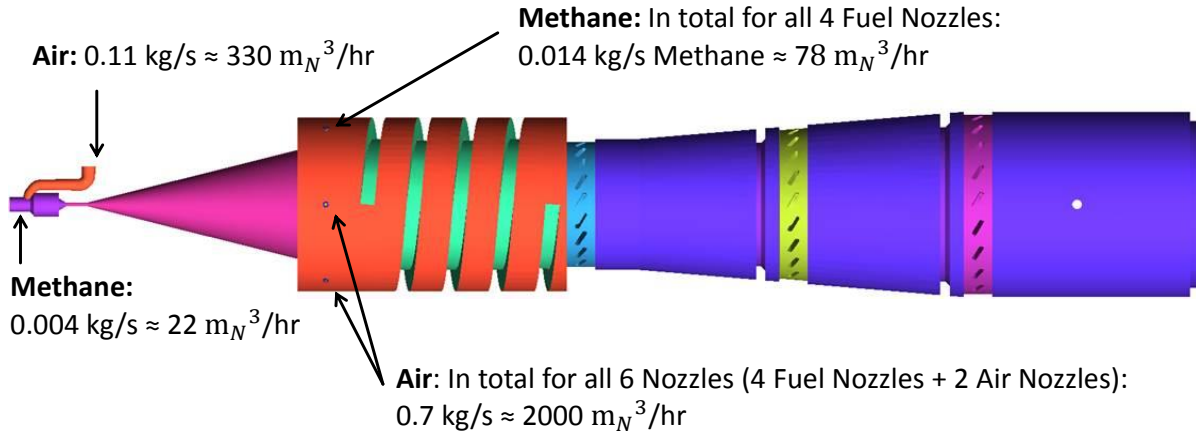From the simulation results presented in the second report, three main issues have been identified:

1. The spiral inside the combustion chamber does not provide any swirl to the fluid flow. Instead, recirculation zones are formed at the spiral's edges. Therefore, the spiral should be replaced by swirl generators.

2. The air nozzle diameter, as well as the fuel nozzle diameter (see Figure 1), are quite small compared to the burner's dimensions. This limits the air and fuel flow rates, resulting in a low thermal output of presently 325 kW (when using methane). The overall air to fuel ratio should be stoichiometric or slightly fuel lean to avoid soot formation.

3. The purpose of the inner pipe is not quite clear. As the flow through the pipe is restricted, no additional swirl for mixing and burn-out is created by the pipe.

Based on these results and a discussion during a video-connference on 2nd of December and follow up e-mail correspondance a new version of the CFI combustor and corresponding boundary conditions and flow rates have been agreed for the next step of the simulations. This geometry of the combustor and of the single parts together with the volumetric flow rates of the air flows and fuel flows have been transmitted to Ing. de la Sovera by 22nd of December. The operating conditions of this version are approximately 1 MW thermal power using only Methane as fuel. The combustion chamber was equipped with six injector nozzles, four of them being fed with fuel and air and two of them being fed by only air. The thermal power and the fuel and air flow rates are set to obtain a combustion temperature of approximately 1200 degree centigrade to keep the NOx-level low. **This version of the CFI burner is denoted setup E**.

2 NEW GEOMETRY, FLOW RATES AND BOUNDARY CONDITIONS FOR CFI SETUP E

An overview over the new geometry of CFI burner setup E and the corresponding flow rates and boundary contitions is given in figure 2. All dimensions of the nozzles, the injector, burning chamber, swirl generators and side nozzles have been extracted from the detailed drawings handed to Prof. Bockhorn by Dr. Baccino during his visit in Karlsruhe on 2nd of December 2015. The thermal output of this version is now about 1 MW using Methane as fuel. The fuel may be replaced in future simulations by other kinds of fuels which may be supplied through the single nozzles. The spiral placed inside the combustion chamber has the function of a heat storage so that re-ignition in case of extinction of the flames is enabled. For that reason the spiral has been retained. The spiral placed inside the combustion chamber can be identified by the green surface and the swirl generators placed in the downstream part of the combustion chanber are indiceted by different colors (blue, yellow and magenta). More details of the geometry are given in the section 3.

Thermal Output 1 MW

Air: 0.11 kg/s ≈ 330 $m_N{}^3$/hr

Methane: In total for all 4 Fuel Nozzles: 0.014 kg/s Methane ≈ 78 $m_N{}^3$/hr

Methane: 0.004 kg/s ≈ 22 $m_N{}^3$/hr

Air: In total for all 6 Nozzles (4 Fuel Nozzles + 2 Air Nozzles): 0.7 kg/s ≈ 2000 $m_N{}^3$/hr

In total: 0.018 kg/s Methane + 0.81 kg/s Air → Fuel–air equivalence ratio φ ≈ 0.4
Adiabatic Flame Temperature ≈ 1200 °C

Figure 2: *Longitudinal view of the new burner geometry used for the simulations given in the following 2015 (denoted setup E)*

The over all flow rates of fuel and air are adjusted so that an over all lean flame is obtained. The purpose of this is to keep the combustion temperature below 1200 degree centigrade and the formation of NOx correspondingly at low levels. The applied model for describing the formation of NOx is given also in the section 3.

3   NUMERICAL METHOD, COMPUTATIONAL GRID, NO-FORMATION MODEL

3.1   SUMMARY OF THE NUMERICAL METHOD

As decribed in the first report from June 10$^{\text{th}}$ 2015 the system of governing equations cannot be solved analytically. In order to solve it numerically, the differential equations first have to be transformed into algebraic equations. This is done by applying a discretization method, whereby the solutions are approximated only at discrete points in space (and time). Therefore, a computational grid (*mesh*) has to be provided that defines the positions of these discrete points. The discretization method used by CFX is a *Finite Volume Method* based on the *Finite Element Method* called *Element Based Finite Volume Method*. The construction of the computational grid is a very tedious process and has been presented also in the first report from June 10$^{\text{th}}$ 2015. The construction of the mesh has to be performed for every setup of the combustor a new.

The computational grid used for this simulation of the setup E consists of about 9 million elements, most of which have a tetrahedral shape. When changing the dimensions of nozzles, pipes etc. the grid has to be adapted accordingly. For clarity and illustration some parts of the numerical grid are given in figures 4 to 6.

A full run on this grid takes about 450 CPU hours. The simulations were performed on the computing cluster of the Division of Combustion Technology at the Engler-Bunte-Institute. To execute the simulation in parallel, the computational domain is decomposed into smaller sections and distributed onto the CPUs of the cluster.

In addition to the computational grid the boundary conditions of the computational domain (i.e. the operatig condition of the CFI burner) have to be specified. In this simulation, there
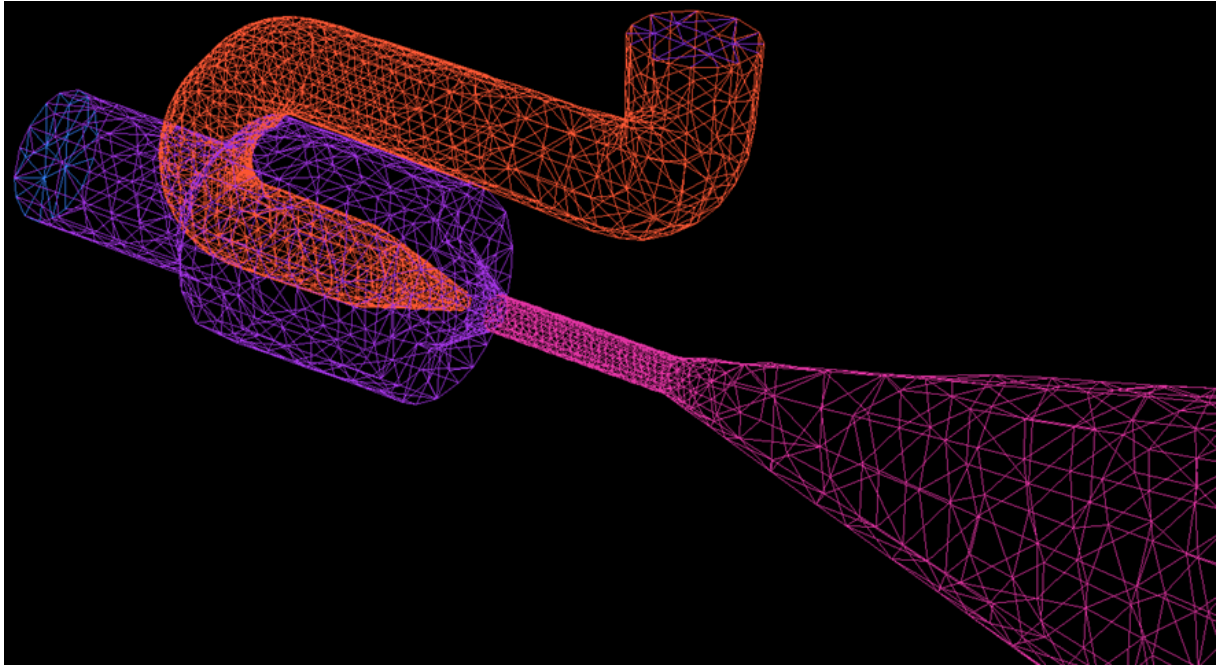
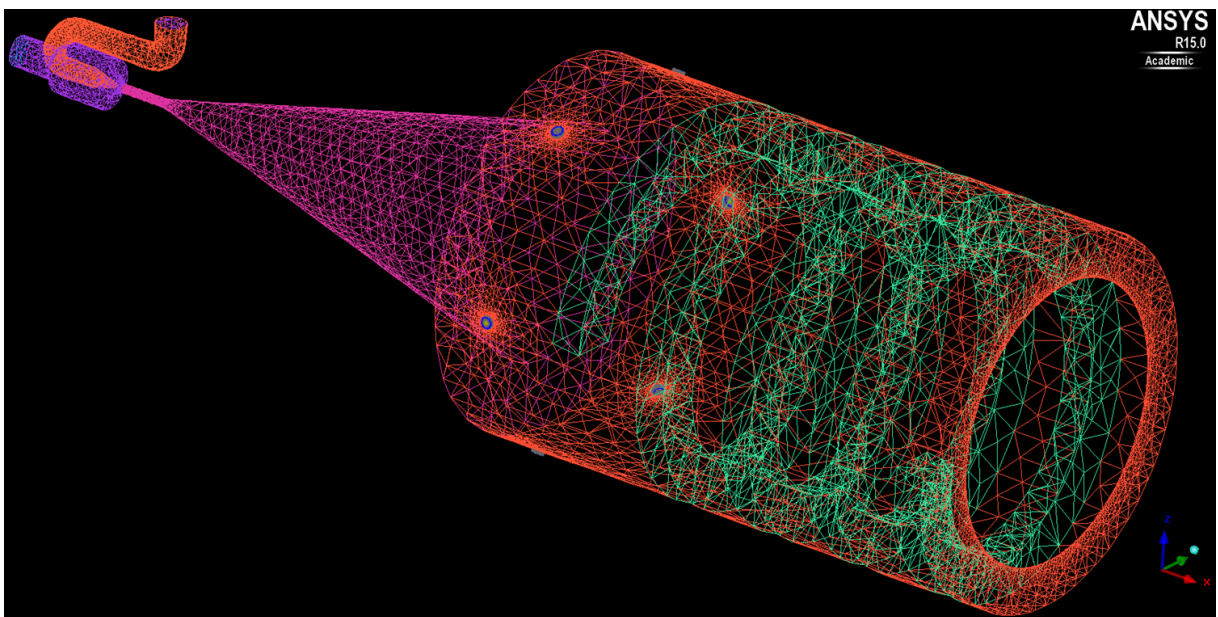**Figure 3:** *Numerical mesh for the injector part of setup E.*

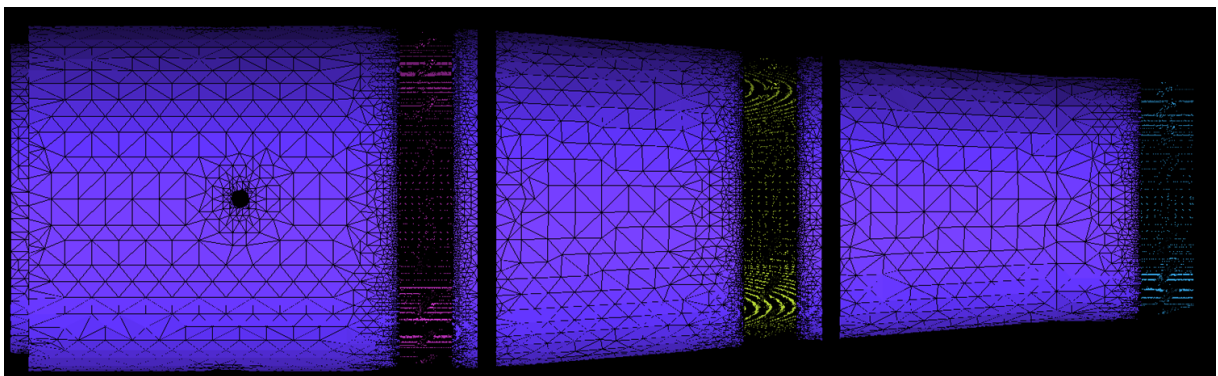**Figure 4:** *Numerical mesh for the primary combustion chamber of setup E.*

Figure 5: *Numerical mesh for the secondary combustion chamber of setup E.*

Figure 6: *Numerical mesh for the swirl generators of setup E.*

are two types of inlets: The inlet into the injector (air and fuel) and the inlet the six nozzles of the primary combustion chamber. Four of these nozzles are fed with methane and two of them with air. All fluids entering the domain as well as the burner environment have a temperature of 300 K. The burner walls are assumed to be adiabatic. The pressure of the burner environment is 1 atm except in the injector. At the inlets, the fluid mass flow rates are set as given in figure 2. The fluid velocities U are then calculated by

$$U_{inlet} = \frac{\dot{m}_{inlet}}{\bar{\rho} A} \tag{1}$$

A is the inlet area and $\dot{m}$ the mass flow rate. The velocity direction is the surface normal to the inlets. The detailed dimensions of all parts have been taken from the detailed drawings transmitted to Prof. Bockhorn by Dr. Baccino during his visit in Karlsruhe on 2$^{\text{nd}}$ of December 2015.

At the walls, the velocity is set to zero to ensure the no-slip condition. The air is assumed to be composed of $Y_{O_2} = 0.233$ and $Y_{N_2} = 0.767$. At the inlets, the mass fractions are fixed - the air inlet has the air composition, whereas the fuel inlets (injector and side inlets) have a fixed value of $Y_{CH_4} = 1$.

As a first approach, the turbulent intensity I at all inlets is set to 5 %. The turbulent kinetic energy $\tilde{k}$ and $\tilde{\omega}$ are calculated by:

$$\tilde{k}_{inlet} = \frac{3}{2} I^2 U_{inlet}^2 \tag{2}$$

$$\tilde{\omega}_{inlet} = \bar{\rho} \left(1000 \cdot I \mu \right)^{-1} \tag{3}$$

The flow near the walls is additionally modeled by wall functions: Because the computational grid cannot fully resolve the viscous sublayer, empirical formulas are used to describe the trans-

port processes in wall near regions. The method used by CFX blends between scalable wall functions and ω-based models (for details, see the CFX documentation).

To obtain adequate initial values for the simulation, some preceding simulations have been performed:

- The first step is a simulation on a coarse grid using first order discretizations with the *Eddy Breakup Model*. This is done to ignite the gas in the combustion chamber.

- Then, still using the coarse grid and first order discretizations, an approximate solution with the *Finite Rate Chemistry* approach is created.

The final results with the coarse grid are then used as initial values for the ultimate simulations with the finer grid with about 9 million elements and the setup summarized below:

- the ultimate simulation is done using the stationary 3D RANS method and the SST k-ω turbulence model.

- a second order discretization scheme for the advection terms is applied.

- combustion is modeled by the Finite Rate Chemistry approach using a single-step reaction for methane as fuel.

- the computational grid consists of about 9 million elements. Because of this and the inclusion of the formation of NO which necessitates the solution of an additional balance equation (see section3.2), each simulation takes about 450 CPU hours.

- the fluid is a compressible and ideal gas, as well as an ideal mixture.

3.2   NO-Formation Model

To simulate the formation of NO, an additional balance equation for NO is solved. The source term of this transport equation (formation rate of NO) is split into formation of thermal and prompt NO and expressed as a one step chemical reaction with reaction rate coefficients according to Arrhenius:

$$\dot{\omega}_{\text{NO}} = \dot{\omega}_{\text{NO, thermal}} + \dot{\omega}_{\text{NO, prompt}} \tag{4}$$

with

$$\dot{\omega}_{\text{NO, thermal}} = k_{\text{thermal}} \cdot [O_2]^{\frac{1}{2}} \cdot [N_2] \tag{5}$$

and

$$k_{\text{thermal}} = 4.52414 \cdot 10^{15} \cdot M_{NO} \cdot \exp\left(-\frac{69466\ K}{T}\right) \tag{6}$$

and

$$\dot{\omega}_{\text{NO, prompt}} = k_{\text{prompt}} \cdot [O_2]^{\frac{1}{2}} \cdot [N_2] \cdot [CH_4] \cdot \left(\frac{\bar{M}}{\rho}\right) \tag{7}$$

and

$$k_{\text{prompt}} = 6.4 \cdot 10^6 \cdot M_{NO} \cdot \exp\left(-\frac{36510}{T}\right) \tag{8}$$

where M_{NO} denotes the molecular weight of NO and $\bar{M}$ the mean molecular weight.

Instead of computing these source terms directly during the simulation, a presumed probability density function (pdf) (for both thermal and prompt NO) is used to calculate weighted averages of the rate coefficients:

$$\tilde{k} = \frac{1}{T_{\text{upper}} - T_{\text{lower}}} \int_{T_{\text{lower}}}^{T_{\text{upper}}} k(T) pdf(T) dT \tag{9}$$

where the $pdf(T)$ is a presumed probability density function with the shape of a β-function. The β-function is defined by its mean and variance, therefore, $pdf(T)$ is computed from mean temperature and variance of temperature. By this, an additional balance equation for the temperature variance $(\widetilde{T''^2})$ has to be solved to account for the effect of turbulent fluctuations on the formation of NO.

4 Simulation Results

4.1 Flow Field and Temperature Field Inside the Combustion Chamber

Figure 7 gives the velocity field in the longitudinal plain of symmetry in the middle of the combustion chamber. As can be seen from the figure, the injector nozzle creates high flow velocities. The same can be seen from the side nozzles where air and fuel, respectively, is injected. Downstream of the side nozzles the velocity decreases and is modified in value and direction by the swirl generators. The injector causes a slightly asymmetric velocity field due to the curvature of the pipes for air supply, compare figure 3. This slight asymmetry is pertained in the downstream direction as can be seen from the temperature field given in figure 8.
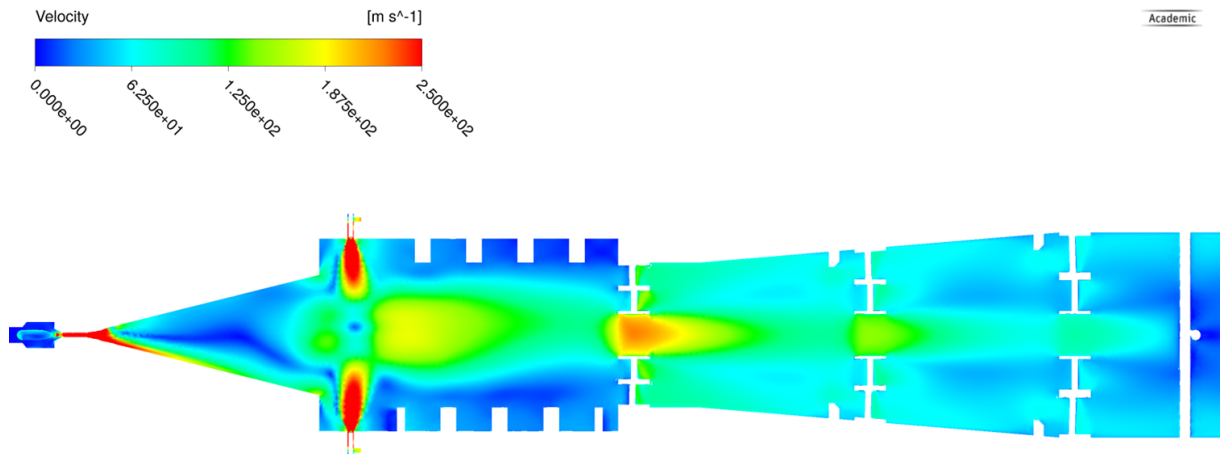

Figure 7: *Velocity field inside the combustion chamber for setup E. The colors indicate the magnitude of the velocity (compare scale in the upper part); the plot refers to the plain of symmetry in the middle of the combustion chamber*

.

The temperature in the diffusor is about 1500 K and the temperaure field is as well somewhat asymmetric due to the asymmetric velocity field. Further downstream in the combustion chamber, where additional air is admixed to obtain an over all lean combustion, the temperature attains values of about 1200 K as estimated by the prescribed inlet conditions. The temperature field in the downstream part of the combustion chamber is homogenized by the swirl generators.

In figure 9 the reaction rate for methane combustion is plotted. The figure clearly indicates the combustion zones of methane in the diffusor where methane and air from the injector are mixed and in the vicinity of the side nozzles, where methane is added.

Figure 10 gives the fields of velocity, temperature, CH_4 mass fraction and NO mass fraction in the cross section of the side nozzles. The velocity and CH_4 mass fraction fields contain also streamlines of the flow. As can be seen from the velocity field (upper left) the fluids from the side nozzles enter the combustion chamber perpendicularly to the wall and combine with the upcoming hot flow from the diffusor forming a counter clockwise rotating super vortex. The secondary fuel of Methane is injected through four pairwise nozzles from the side wall of the

combustion chamber and is intermixed with the secondary air from the two opposite nozzles in the wall and the hot flow (lower left). The temperature profile (upper right) exhibits the higher temperature of the upcoming hot flow from the diffusor and the intermixing of air and methane with this hot flow. Due to the non symmetric flow field of the upcoming flow the temperature in this cross section is not homogeneous and the temperature is higher in the right part of the combustion chamber (upper right). This leads as a consequence to a higher NO concentration in this part of the combustion chamber (lower right).
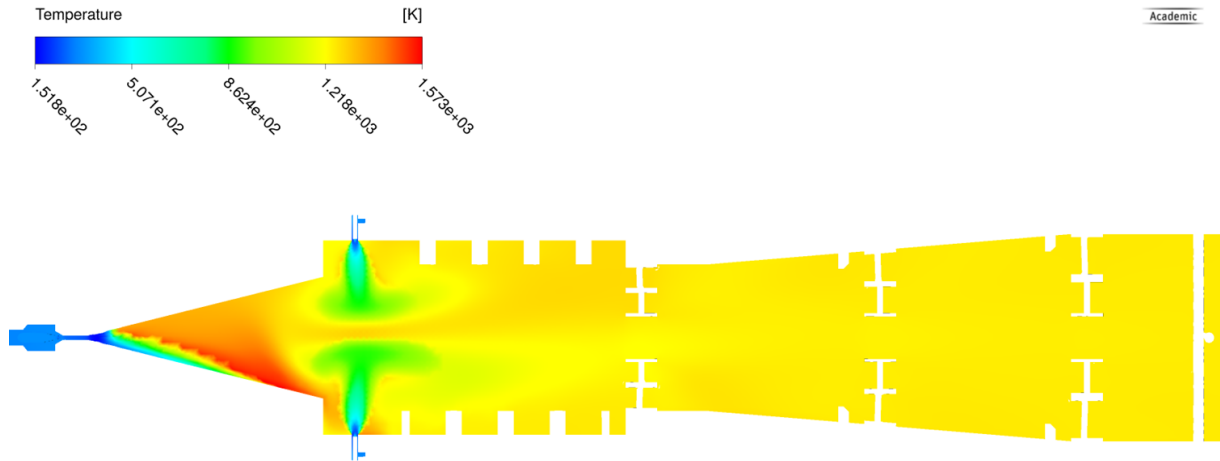

Figure 8: *Temperature field inside the combustion chamber for setup E. The colors indicate the magnitude of the temperature (compare scale in the upper part); the plot refers to the longitudinal plain of symmetry in the middle of the combustion chamber.*
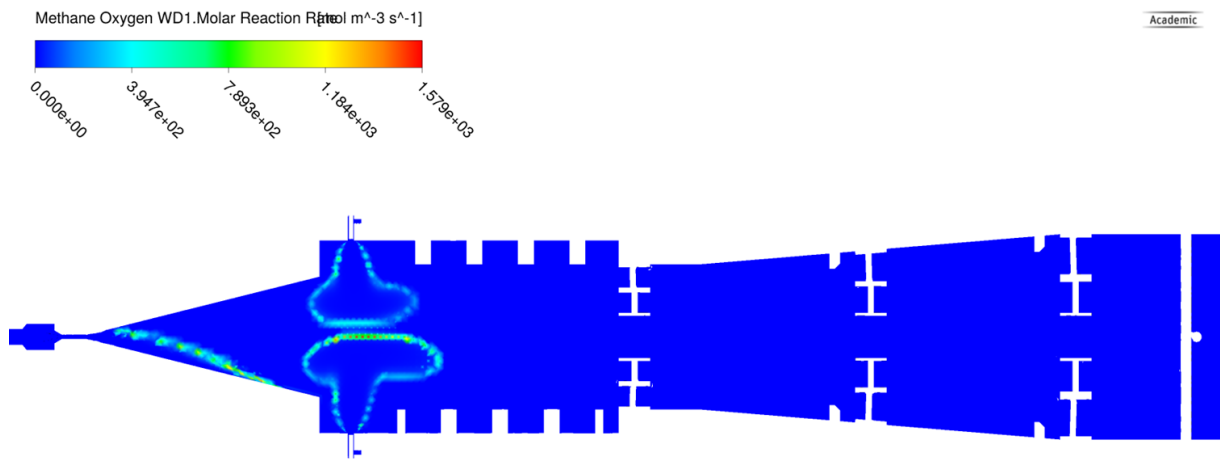

Figure 9: *Field of reaction rate for methane combustion inside the combustion chamber for setup E. The colors indicate the magnitude of the reaction rate (compare scale in the upper part); the plot refers to the longitudinal plain of symmetry in the middle of the combustion chamber.*

The NO concentration is homogenized in the downstream region of the combustion chamber in the exit region. The exit mass fraction of NO calculated by the NO-model given in section 3.2 is approximately $3 \cdot 10^{-8}$ under these conditions. The mass fraction profiles in the longitudinal plain of symmetry in the middle of the combustion chamber are displayed in figure 11.

Finally, in figure 12 the temperature field in the longitudinal plain of symmetry of the combustion chamber illustrated with the corresponding streamlines is displayed (lower part). In the uper part a three dimensional picture of the streamlines in the combustion chamber is given including the geometry of the combustion chamber. The displayed parts of the combustion
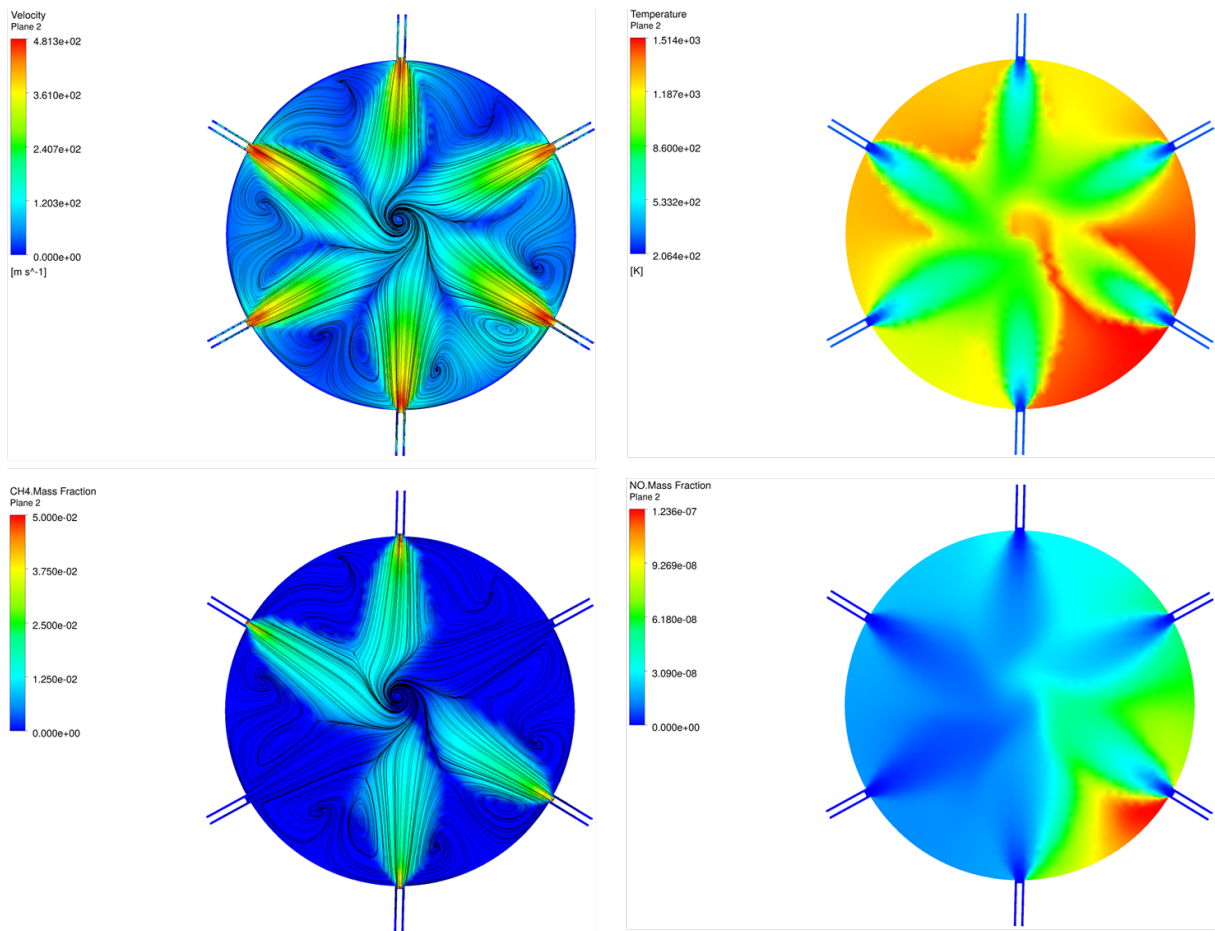
Figure 10: *Field of velocity, temperature, CH_4 mass fraction and NO mass fraction in the cross section of the side nozzles for setup E. The colors indicate the magnitude of the respective quantities (compare scales).*
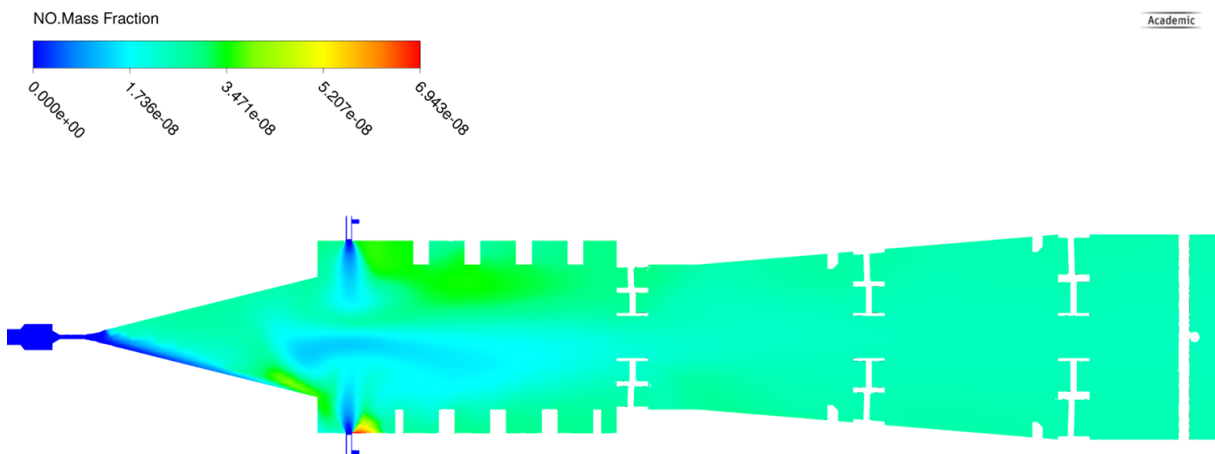

Figure 11: *Field of NO mass fractions inside the combustion chamber for setup E. The colors indicate the magnitude of the NO mass fraction (compare scale in the upper part); the plot refers to the longitudinal plain of symmetry in the middle of the combustion chamber.*
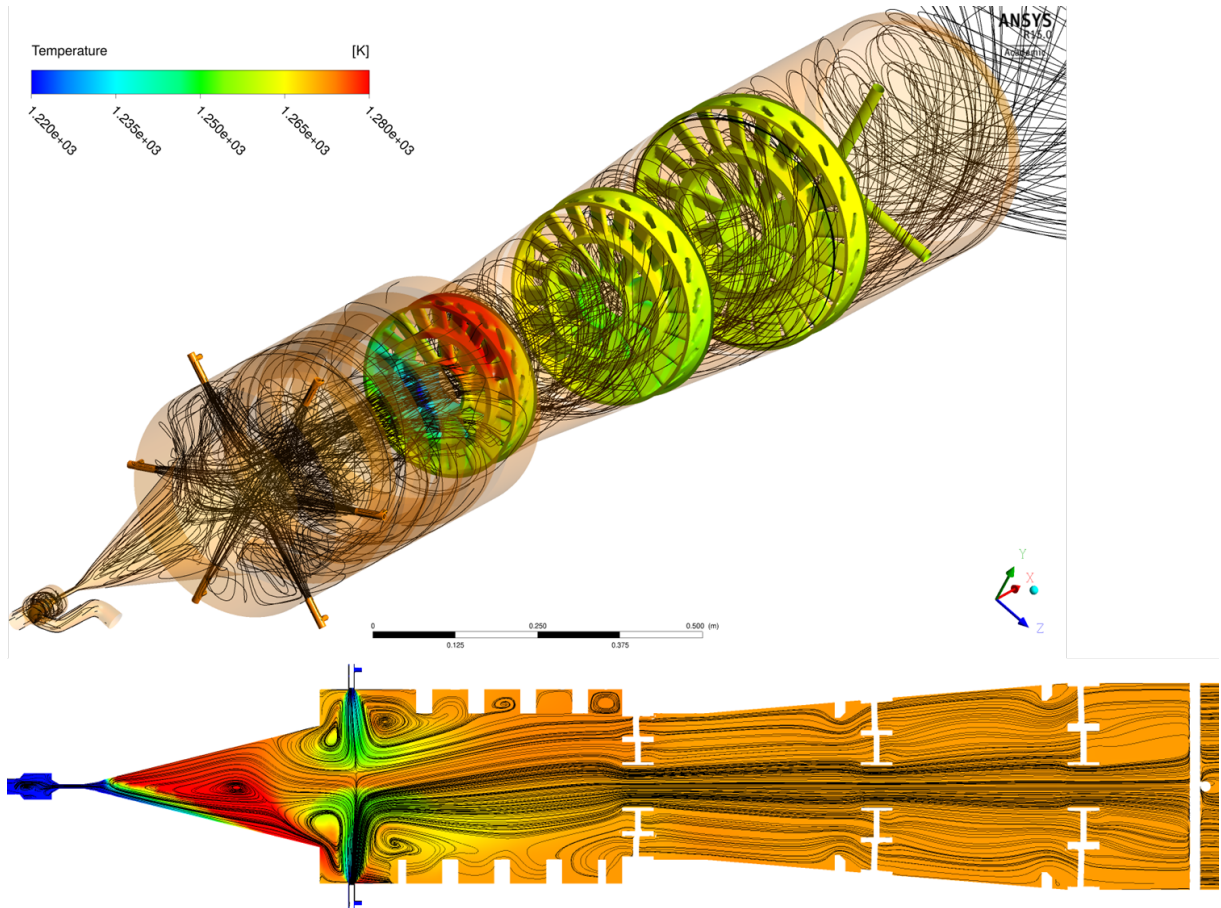
9

Figure 12: *Field of the temperature inside the combustion chamber for setup E overlayed by the corresponding streamlines (lower part, the plot refers to the longitudinal plain of symmetry in the middle of the combustion chamber); three dimensional pictures of stramlines in the combustion chamber(upper part).*

chamber are underlayed with the temperature. The figure conveys an over all view of the flow field and the combustion occuring within the setup E.

5   Conclusion

Based on the simulation results presented above for the stup E of the CFI combustor, the following conclusions may be drawn:

1. The new geometry of setup E apparently is a version which garanties complete burn out of the fuel (in this case Methane, other fuels have to be simulated in future work).

2. The temperature within the combustion chamber can be controlled by the ratio of the flow rates from the injector and the side nozzles. A further possibility of control is the number of side nozzles fed with fuel or air.

3. The slightly asymmetric flow field and as a consequence the asymmetric temperature field in the combustion chamber, which has a negative effect on the NO formation in the combustor, may be avoided by a changed design of the injector.

Setup E apparently is a further approach to the stepwise approximation of a version of the CFI burner with realistic operating conditions. Changes in geometry will be realized in further simulations. Also, the fuel may be replaced in future simulations by other kinds of fuels which may be supplied through the single nozzles.